The Evolution of Raindrop Spectra: Comparisons between Modeled and Observed Spectra along a Mountain Slope in Switzerland

ZEV LEVIN, GRAHAM FEINGOLD, SHALVA TZIVION

Department of Geophysics and Planetary Sciences, Raymond and Beverly Faculty of Exact Sciences, Tel Aviv University, Ramat Aviv, Israel

ALBERT WALDVOGEL

Atmospheric Physics ETH, Zurich, Switzerland

(Manuscript received 2 July 1990, in final form 5 December 1990)

ABSTRACT

A comparison is made between the evolution of raindrop spectra as measured at stations in the Swiss Alps separated by vertical distances of the order of 600 m, with that modeled in an axisymmetrical model including detailed microphysics. Results show that under steady rain, weak advective conditions, and rain rates greater than 2 mm h^{-1}, the model satisfactorily reproduces the features of the observed drop spectrum. Results deteriorate for low rain rates (of the order of 1 mm h^{-1}) since drop collisions are too few to modify the spectrum significantly. The general agreement between modeled and observed spectra suggests that further considerations of this kind are justified.

1. Introduction

The problem of raindrop spectra evolution has been analyzed from a theoretical point of view by numerous authors (e.g., Srivastava 1971; Gillespie and List 1978/79; Valdez and Young 1985; List et al. 1987; Tzivion et al. 1989). The question arises as to how well these numerical simulations of rainfall compare with natural rainfall conditions. While field observations do abound (e.g., Willis 1984; Feingold and Levin 1986; Steiner and Waldvogel 1987), they are generally unsuitable for comparison with model results. Airborne measurements suffer from poor temporal and spatial resolution as well as the disadvantage that measurements at different altitudes are not coincidental. Ground measurements have good time resolution but normally do not show resolution with altitude. In a paper by Gori and Joss (1980) (hereafter GJ), the authors compared spectra sampled at three stations located at different altitudes, the highest and the lowest stations being separated by nearly 800 m of fall. The data were collected at Mount Cardada in southern Switzerland. After precluding possible instrument bias, the authors showed how both long-time-averaged spectra and instantaneously averaged spectra differ slightly, but noticeably, from one station to the next.

The work by GJ infused the idea of performing a comparison of their observed spectra with model results of evolution through collision/coalescence, breakup, and evaporation. The model used is an axisymmetrical rainshaft model presented in Feingold et al. (1991). The model will only briefly be described here. The dynamical framework is hydrostatic and has open boundaries. In all, five prognostic equations are solved; one for the vertical wind speed, two for thermodynamic parameters giving humidity and temperature perturbations, and two equations for the drop-number and drop-mass concentrations is a spectral category. The radial velocity is determined from the equation of continuity. The model includes detailed warm microphysics (see Tzivion et al. 1989). The drop spectrum is divided into 33 categories, and 2 moments of the category distribution function (number and mass concentration) are solved for in each category. In the model simulations, only the precipitating stage is considered. Initial temperature and humidity profiles are given, and the model is then initiated by providing a source of rain somewhere in the domain.

Since this rainshaft model does not include the affects of topography, it is first necessary to consider just how feasible a comparison between observed and modeled evolution would be. The data sampled along a steep slope are necessarily affected by the existence of the mountain obstacle itself and topographically induced dynamic effects would have a major impact. In nonquiescent conditions, under vertical wind shear conditions, the drop spectrum may be determined by the dynamics of precipitation (e.g., wind-sorting effects and the pressure gradient), rather than the microphysical

Corresponding author address: Dr. Graham Feingold, NCAR/MMM, P.O. Box 3000, Boulder, CO 80307.

processes of collision/coalescence and breakup. For example, a prevailing horizontal wind of magnitude u may induce an updraft w whose magnitude is proportional to $u \tan\alpha$, (α being the angle of the mountain slope). For steep Alpine slopes, w may be significant. Updrafts will tend to suspend the smaller raindrops and increase the time available for spectral evolution by decreasing fall velocities. On the other hand, downdrafts generated by the rainfall will increase fall velocities, decrease the time available for evolution, and create divergence when the airflow strikes the mountain barrier.

The complex interaction between the wind field and a nonuniform mountain slope will also result in turbulence. The result, once again, may be that the drop spectra bear little resemblance to our theoretically obtained spectra. Finally, we consider the possibility that upslope winds may create divergence aloft. Smaller drops could be carried up in the updraft, and follow a complex trajectory before falling out to the ground. Also, recirculation of drops could not be ruled out in such a case. Thus, a drop following some complex air motion adjacent to the slope could feasibly grow far larger than under normal quiescent conditions.

In the event that these dynamic effects are dominant, the results are a priori not expected to match since topographical effects are not included in our model. Furthermore, observations made during windy conditions are problematic, not only due to the aforementioned effects but also because of the sensitivity of the distrometer response to strong air movements. The impaction distrometer used in this experiment (Joss and Waldvogel 1967) assumes the drops to be falling at their respective terminal velocities and strong vertical winds will understandably influence the instrument response (Kinnell 1976; Joss and Waldvogel 1977). List (1988) and Sheppard (1990) have conducted further analysis of the distrometer. List has shown how the lower cutoff diameter of the instrument, as well as the dead-time effects increase with increasing rain rate. He concludes that only spectra from steady rainfall should be averaged. (Further reasons for the desirability of steady rainfall are discussed in the following text.) Sheppard shows how deviations from the manufacturer's quoted instrument response can create a tendency to multiple modes in the drop spectrum. These facts should also be borne in mind as potential sources of error.

Another important criterion is the duration of the rain and the temporal correlation between rain rates

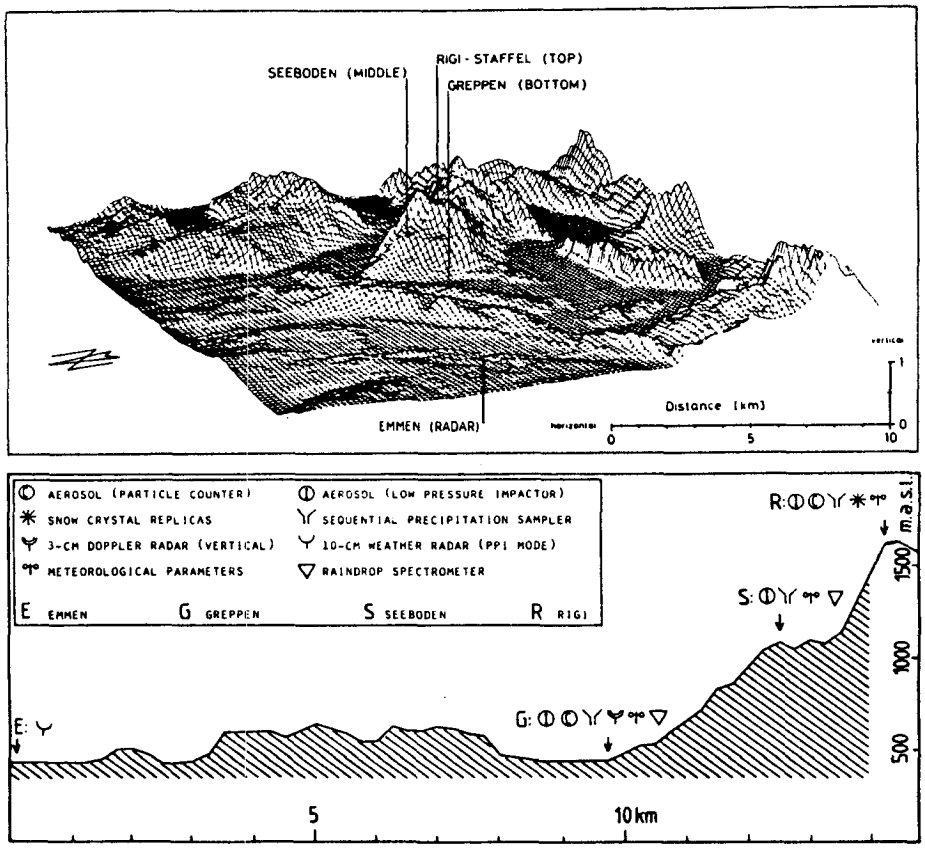

FIG. 1. Location of observation stations at Mount Rigi, Switzerland. Drop-size distribution data are available at stations M and B. (From Schumann et al. 1988.)

at the different stations. Precipitation of sufficient duration and approximately steady rain rates would facilitate comparison. Moreover, for comparison with model simulations, it is best if the rain is widespread enough for lateral differences in precipitation to be negligible. (This point is closely related to the dynamic effects discussed previously.) Lastly, a prerequisite for comparison with the present model is that the precipitation is all (or at least mostly) in the liquid phase.

In the final analysis, any comparison between theoretical and observed drop-spectra evolution must be judged in terms of the inherent limitations of both the model and the observations. Thus our aim here is to establish whether the trends in evolution are consistent, and, in any event, to try to point out possible causes for discrepancies—qualitative or quantitative. In the present paper, we will implement the dynamical rainshaft model presented in Feingold et al. (1991) to trace the evolution with altitude of raindrop spectra. The model results will then be compared to the observations made at stations separated by vertical distances of the order of 600–800 m. Two datasets will be used; the first, data from Mount Rigi, Switzerland, (see Schumann et al. 1988) and the second, results presented by GJ from Mount Cardada, Switzerland.

2. Results and Discussion

a. Mount Rigi

The Atmospheric Physics group at ETH has sampled data along the slopes of Mount Rigi, with the aim of studying the problem of aerosol scavenging by precipitation. Meteorological data are available at three stations (top, middle, and bottom) at altitudes of 1620, 1030, and 430 m, respectively (Fig. 1), and include temperature, relative humidity, and pressure measurements. These stations will be referred to as stations T, M, and B, respectively. Two distrometers supply 1-min averaged spectra at station M (1030 m) and station B (430 m). The raw distrometer data pertaining to three storms exhibiting approximately steady rain of long duration were made available to us. Only one of these storms 19 March 1986 was chosen on account of the fairly low recorded wind speeds (<2 m s^{-1}) and reasonable correlation between rain rates at the two stations. Furthermore, the steady nature of the rainfall and low rain rates (see Fig. 2) provided us with confidence in the quality of the distrometer measurements. A full description of the event can be found in Schumann et al. (1988). It would be feasible to study the other two cases in the future if a slab-symmetrical version of the model, which would include wind shear and topography, were used.

On the day in question, the temperature at the top station (1620 m) was a little above 0°C at 1600 (local time) when rain of significant rates had commenced. From the observed lapse rates of temperature it is expected that the melting level was at about 1400–1600 m MSL during the first few hours of the storm. Although most of the precipitation reaching station M is expected to be in the liquid phase, the possibility of the existence of partially melted snow and small graupel cannot be ruled out. Partially melted graupel particles are expected to be recorded by the distrometer according to their equivalent drop size. However, the relatively slow fall velocities of snow particles (compared to drops of equivalent mass) would mean that they would be recorded by the distrometer as smaller drops. Since the model does not include the ice phase, we cannot rule out possible error in the comparisons due to this effect.

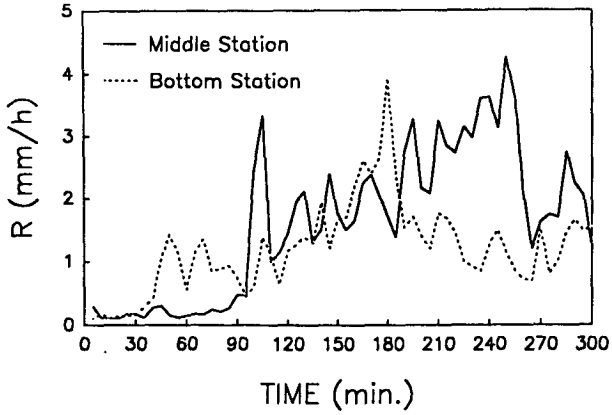

FIG. 2. A comparison of 5-min–averaged rain rates as a function of time as measured by the distrometers at stations M and B. Correlation is reasonable (0.56) with a phase delay of 4–5 min. The time series begins at 1600 h.

The distrometer data were processed using the procedures presented in Feingold and Levin (1986). Spectra observed at the two stations were averaged over a period of 321 consecutive minutes of rain. Although precipitation on the day in question was of much longer duration, only 321 min of synchronous measurements were available. A plot of rain rate versus time at stations M and B is shown in Fig. 2. Analysis shows that the correlation is fair and has a maximum value of 0.56 with phase delay of 4–5 min. Since the distance of fall between the two stations is 600 m, this implies fall velocities of the order of 2–2.5 m s^{-1}. In the simulations that follow, the spectra used as input to the model will have rain-rate–weighted averaged drop sizes whose terminal velocities are in accordance with these "observed" fall velocities.

Rain rates at the middle station tend to be greater than those at the bottom; the average rain rate at M is 1.9 mm h^{-1} compared with 1.33 mm h^{-1} at B. This fact precludes the use of a fixed dynamical model for simulating the rain because rain rate is conserved with altitude (in the absence of evaporation) there. Since rainfall is defined as the flux of a volume of water, the decrease could conceivably occur if the subcloud wind field is divergent, and the volume of water spreads over a larger surface area as it falls. Alternatively, the loss

could be accounted for by evaporation. Although the rainfall duration is over 5 h for this dataset, measurements of RH at station B are typically of the order of 95%. The reason for this could be that the weak downdrafts generated by the falling rain create compressional warming, which is sufficient to offset the evaporative cooling and maintain subsaturation. Alternatively there could be other local effects.

Thus we chose to use a fairly high-resolution (60 $\times$ 40 m^2) version of the dynamic model to simulate the rainfall. Higher resolution (30 $\times$ 20 m^2) is possible but extremely costly because the time required for a steady state to be achieved for spectra with such low rain rates is in the order of *hours*. Various methods of comparing the observed evolution with modeled evolution were considered. The most rigorous test would be to vary the input to the model, (using the observed spectra at station M), and to attempt to reproduce the temporal evolution of the spectra at the lower station, at the 1-min resolution of the distrometer measurements. The other approach would be to attempt to simulate the *average* trends in evolution, i.e., to compare the average drop spectrum aloft with that lower down the mountain slope. This was the approach of Gori and Joss (1980). In keeping with the motivation of this paper and bearing in mind the various possible sources of error discussed in section 1, we have opted to compare the average trends in evolution rather than the detailed temporal changes. It is recognized that the evolution of the average spectrum is not identical to the averaged evolution of each individual spectrum. An attempt to alleviate this has been made by partitioning the data according to rainfall rates. This will be elaborated upon in the forthcoming discussion.

Because of the short fall distance separating stations M and B, it was decided to include only spectra having rain rates of over 2 mm h^{-1}. Spectra having low rain rates vary considerably in form (e.g., Feingold and Levin 1986), and their presence in the dataset would tend to mask the evolution of the heavier precipitation. In addition the rate of evolution of these spectra is too small to be useful for comparison (Rogers 1989). The average spectra at stations M and B are shown in (Fig. 3a) and comprise 140 and 43 individual spectra, respectively. The average rain rate at M is 2.92 mm h^{-1} compared to 2.62 mm h^{-1} at B, with the decrease probably being due to divergence and evaporation. The difference in the spectra is marked with the spectra at M showing a smaller component of large drops and a larger component of small drops compared to the spectrum at B. We note that the rain-rate–weighted average diameter is in the order of 0.8 mm which implies a fall speed of 3.3 m s^{-1}. This translates to a time lag of 3 min for the 600-m fall distance. (Remember that

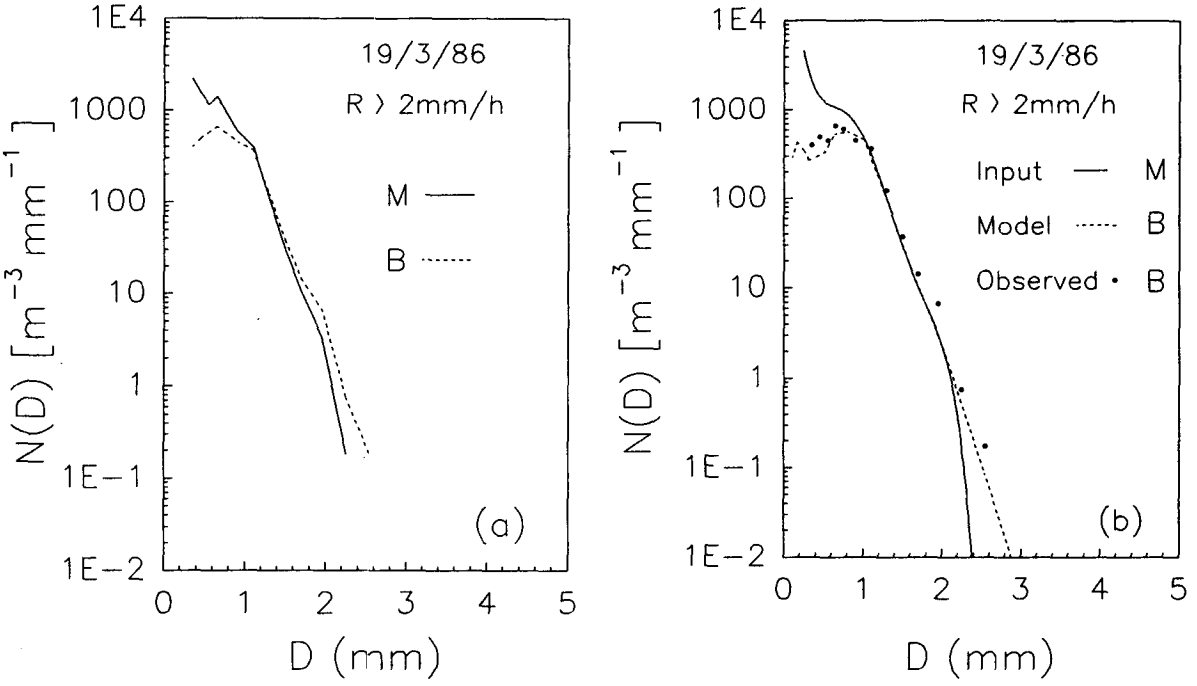

FIG. 3. (a) A comparison of average spectra observed at stations M and B. Only rain rates greater than 2 mm h^{-1} have been included. (b) A comparison between observed and modeled evolution of drop spectra. The curve marked *Model* is a polynomial fit to the observed data points at station M and is used as input to the dynamic model. The dotted line represents the spectrum obtained by the model after 600 m of fall. The data points correspond to the average spectrum observed at station B. Note the good overall fit of the model predicted evolution to the observed evolution. Model predicted growth of larger drops is a little slower than observed.

for the entire dataset, which included many events at lower rain rates, the maximum correlation was at a lag of 4–5 min.)

As input to the model, we use the average spectrum at station M presented in Fig. 3. However, since the distrometer size categories are not coincident with the model drop-size bins, it was necessary to perform an interpolation. This was done using a high-order polynomial, the order of which was determined by its ability to reproduce the fine features of the data. This polynomial fit to the data was then used as input at the top of the rainshaft and over the entire radius (750 m) of the rainshaft. Various forms of interpolation were tried but the results were not sensitive to this factor. The observed profiles of temperature and humidity just prior to the onset of significant rain were used as initial conditions for the model. The microphysical processes of collection/breakup and evaporation were included and the model was run for 1 h and 40 min, by which time the raindrop distribution was seen to be approaching a steady form. The evolution of the spectrum is shown in Fig. 3b. The model succeeds in reproducing the growth of the larger drops with perhaps surprising accuracy. In the region 0.8–1.5 mm the fit is very good. Below 0.8 mm, the model tends to slightly underestimate the drop concentration. This is more marked at about 0.4 mm where the observed concentration is about twice that of the modeled concentration. However, both the observations and the model results predict a peak at about 0.65 mm. For diameters less than 0.35 mm there is no basis for comparison because this diameter is the lower cutoff of the distrometer. Above 1.5 mm, the model predicts the growth of larger drops fairly well but tends to underestimate the rate of their production. Note also that the model generates drops larger than 2.55 mm. These drops were not observed but since their concentration is so low it is possible that they did exist, but were not registered by the distrometer with its small sampling area (50 cm^2).

Figure 4 shows the temporal evolution of the spectrum at the ground station. Note how after 1 h the tendency for depletion of the smaller drops is clearly visible and growth of the larger drops is evident. As expected, evolution is slow at these low rain rates.

For the full 100-min simulation, the modeled decrease in rain rate is about 15% compared to the observed decrease of 10%. A look at the relative humidity near the ground shows values of about 90%, which falls in the range of the observed values. The field measurements show that an RH of close to 100% at the base station was only achieved after about 3 h of rain, during which time the air temperature had dropped from about 10° to 6°C, mostly due to radiative effects and small-scale phenomena (vertical mixing, Schumann et al. 1988). Since the model does not include facilities for the aforementioned effects and cannot simulate rain (at high resolution) for periods of more than about 1 h and 40 min, we do not wish to place too much emphasis on the model's ability to simulate all the aspects of this long duration storm. In general, however, the overall comparison between observed and simulated rainfall is pleasing.

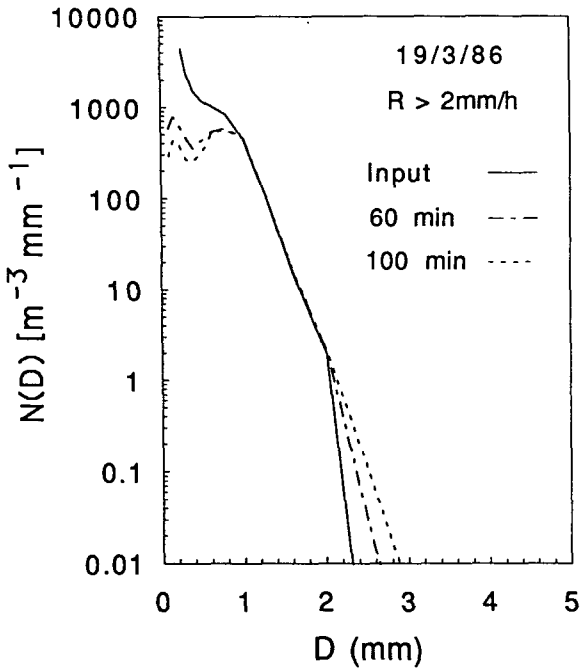

FIG. 4. Model produced spectra at the ground after 60 min and after 100 min for the same input as in Fig. 3b. The bimodality in the spectrum is already evident after 60 min. However, the evolution toward steady state is, as expected for these low rain rates, slow.

In spite of the good agreement obtained in the previous case, it was decided to perform another simulation. This time all rain rates greater than 1 mm h^{-1} were included. In addition, only the rainfall period 1600–1800 h was used since, after this point in time, the temperature began to decrease rapidly as the sun disappeared. Data sampled after this time most likely include a component of snowflakes since they were sampled while the melting level became progressively lower.

The simulation of this case was performed in the same manner as the previous one. The average distribution (for $R > 1$ mm h^{-1}) was used as input to the model for a duration of 1 h and 40 min. This spectrum comprises 86 individual spectra, whereas the average spectrum at the base station comprises 52. The rain rate of the average spectrum at the middle station is 2.01 mm h^{-1} whereas that at B is 1.39 mm h^{-1}. We see in Fig. 5 how the spectrum evolves somewhat differently to the previous case. The spectrum observed at the base station has fewer drops than that at M throughout most of the range. Evolution is not as marked as in the case for spectra comprising only $R > 2$ mm h^{-1}. We also see how the model simulates the observed evolution reasonably well, especially in the

region 1–2 mm. Above 2 mm the model once again shows some growth of larger drops in small concentrations. These drops were not observed by the distrometer at the base station. Below 1 mm, the simulated and observed spectra differ, especially between 0.4–0.6 mm where the model underestimates the observed concentrations by a factor of about 2–3. At 0.35 mm (the lower cutoff of the distrometer) the comparison is a little better. The discrepancies between modeled and observed results may be due to enhanced collection of drops in the region 0.4–0.6 mm by larger drops to create drops >2 mm diameter. Alternatively, evaporation may be removing the small drops at too fast a rate. The model predicts a decrease in rain rate of 34% compared to the 30% observed decrease and a RH of 90% at the base station compared to the observed range of between 88% and 96%. Thus, once again there is good agreement between modeled and observed results.

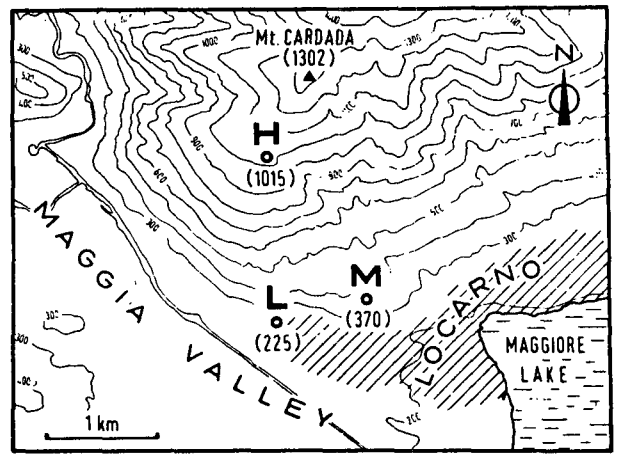

FIG. 6. Location of observation stations at Mount Cardada, Switzerland. Drop-size distribution data are available at stations H, M, and L. (Gori and Joss 1980).

b. *Mount Cardada*

The question now arises as to just how representative the results from Mount Rigi are. The only other results known to us showing the evolution of drop spectra with altitude are those published by Gori and Joss (1980) from Mount Cardada. Their data were sampled in the month of September (28 September 1974) when the freezing level was at an altitude of about 1600 m. The stations are located at altitudes of 1015, 370, and 225 m (Fig. 6) and will henceforth be referred to as stations H, M, and L, respectively. On the day in question, the stations sampled 684 min of continuous rain with an average rain rate of approximately 2 mm h^{-1}. The authors specifically chose an event where observed horizontal wind speeds were low (<0.5 m s^{-1} for 75% of the duration of the rain). However, the winds did on rare occasions peak at 3 m s^{-1} and wind direction changed from westerly during the first part to easterly during the second part of the storm. This fact should be borne in mind to account for possible discrepancies in observed spectra at the different stations. Thus the GJ results fulfill our criteria for comparison satisfactorily. Gori and Joss (1980) present two types of spectra at each station. The first are average distributions for the entire storm, which tend to be exponential due to the summing of many spectra of very different shapes (Joss and Gori 1978). The second are averaged instant spectra representing the average form of a 1-min sampled distribution. The method of averaging is described by Joss and Gori (1978). In order to be consistent with our treatment of the data from Mount Rigi, we will look at the data for long-time averages only.

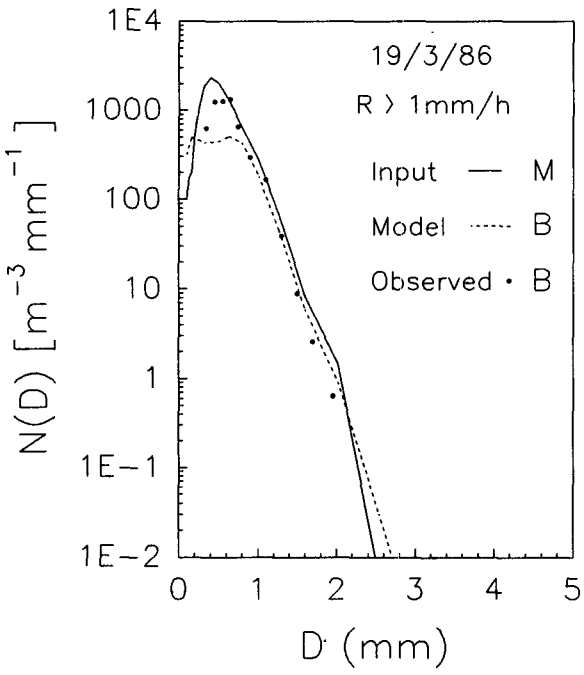

FIG. 5. As in Fig. 3b, but for $R > 1$ mm h^{-1}. The overall fit is good, except for the region 0.4–0.6 mm.

A look at the spectra in Fig. 7a shows how the observed differences in spectra as a function of altitude are small, in fact, far smaller than those observed in the previous case. In contrast to the data from Mount Rigi the average spectrum at the base station has fewer large drops than the station at the top. As was the case with the Mount Rigi data, the average rain rate at the top station is higher than that at the bottom (this time by 18%). Since the raw distrometer data are not available, we have reconstructed the spectra in Fig. 7a using the parameters of the equation given by GJ and used them as input to the model. Having no knowledge of the ambient conditions on the day in question, an initial RH profile of 100%, a ground temperature of 10°C, and a lapse rate of 8°C km^{-1} were assumed. However, results showed little dependence on the choice of the initial conditions.

The curve labeled H in Fig. 7a was imposed at cloud base over the entire radius of the shaft (750 m) and the model was run until a steady state was achieved. The results for this simulation are presented in Fig. 7b together with a comparison with the observed average spectrum at the base station. We see how the curve at station H evolves after 800 m of fall to a bimodal form with fewer drops throughout. Breakup is responsible for reducing the number of the largest drops. At the small-drop end of the spectrum, the loss of drops through collection and evaporation overcomes their replenishment due to fragmentation. Below 0.3 mm there is a sharp decrease in the distribution function predicted by the model. Comparing the model result to the data points associated with the curve at station L in Fig. 7, it becomes clear that the model predicted results are close to the observed results only at drop diameters greater than about 3.5 mm. Below 3.5 mm, the model generally predicts fewer drops than observed. At drop sizes less than 1.8 mm the observed results at station L are higher than those observed at station H. This is not reproduced by the theoretical model. Below 0.8 mm, the departure between modeled and observed results becomes quite marked.

The model shows a 25% drop in rain rate over the fall distance of 800 m compared to an 18% observed drop. Although one is encouraged by the fact that there is some similarity between the observed and modeled evolution, inasmuch as the tail of the large drops is concerned, the discrepancies at smaller drop sizes is puzzling. The reasons for this are not obvious but we do offer a few possibilities.

(i) Factors such as dynamic or orographic effects may be responsible. The abundance of small drops at station L may be due to wind sorting effects due to vertical shear or turbulence along the mountain slope.

(ii) The average spectra in the GJ data comprise many 1-min spectra with very low rain rates. It is known that at low rain rates spectra tend to differ considerably from one another especially as regards to their small-drop component (e.g., Feingold and Levin 1986). This might mean that the average curves given by GJ do not show the evolution at the lower end of the spectrum explicitly enough.

(iii) The method of averaging drop spectra used by GJ may have removed some of the details of the spectrum, which could be essential for correct simulation of the evolution.

(iv) The resolution of the model used here (60×40 m^2) is not sufficient to resolve the trends with sufficient accuracy.

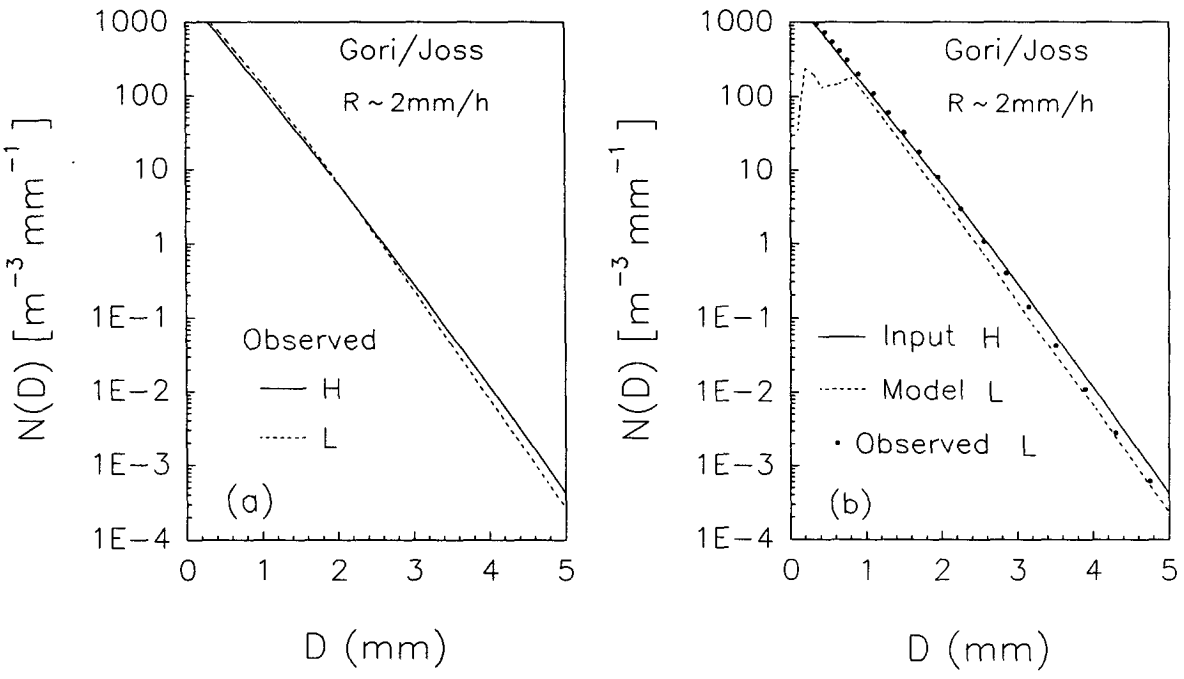

FIG. 7. (a) A comparison of average spectra observed at stations H and L. The curves are average spectra for the entire storm (684 consecutive minutes of rain), irrespective of rain rate. The average rain rate at H is 2.22 mm h^{-1} whereas that at L is 1.82 mm h^{-1}. The spectra have been reconstructed from Gori and Joss (1980). (b) A comparison between observed and modeled evolution of drop spectra. The curve marked *Input* is identical to curve H in (a) and is the input to the model. The dotted line represents the spectrum obtained by the model after 800 m of fall. The data points correspond to the average spectrum observed at station L. Good fit is evident only for drop sizes greater than 3.5 mm. At smaller drop sizes, the model predicts fewer drops than observed.

3. Summary

In this paper we have compared the observed and theoretical evolution of raindrop spectra with fall distance. The model used is the axisymmetrical dynamic model presented in Feingold et al. (1991) including all the warm microphysical processes. The observed spectra were sampled along the slopes of two mountains in the Swiss Alps. Two datasets have been chosen for the comparison. The first, data sampled at Mount Rigi by the atmospheric physics group at ETH comprised raw distrometer data at two stations separated by 600 m in the vertical as well as meteorological data such as temperature, pressure, and relative humidity. The second set of data has been inferred from results published by GJ showing the evolution of spectra at stations separated by a maximum distance of 800 m. Since the raw data were not available for this event, the average spectra presented in that paper have been reconstructed using the equations and parameters presented by the authors. Both events were characterized by low horizontal wind velocities (less than 2 or 3 m s^{-1}), widespread rain at low rain rates, and of long duration and a reasonably high melting level. In both cases the average rain rates measured at the lower station were 10%–30% lower than that at the higher station (600–800 m above).

In both cases, the observed decrease in rain rate is reproduced by the model with reasonable accuracy. In the case of the dataset from Mount Rigi, good agreement between observed and modeled evolution is obtained. The model predicts the growth of larger drops through collection and a decrease in the number of smaller drops through evaporation and collection. In addition, the relative humidity obtained by the model for steady rain during the course of 1 h and 40 min falls within the range of the observed values. On the other hand, the results of the simulation using the results from GJ are not as good. They show agreement for drop diameters greater than 3.5 mm, but poor agreement at drop sizes less than 0.8 mm. In the midspectrum the modeled concentrations are slightly smaller than observed. Possible reasons for these discrepancies have been proposed. These include orographic effects and the fact that the GJ data comprised a large number of spectra with low rain rates. The latter vary greatly in shape and undergo little evolution over a fall distance of 800 m, hence, they are likely to mask the evolution of the spectra with larger rain rates, especially at the small-drop end of the spectrum.

It should be borne in mind that the comparisons made here should be considered in terms of the inability of the model to simulate orographic effects. Although the model includes all the processes of evaporation, sedimentation, collection, and breakup in a full two-dimensional model, it does not include topography and its effect on the dynamic fields. Nor does it make provision for radiative effects that play an important role in modifying the ambient conditions during rain of long duration. Nevertheless, the results presented here are very encouraging. It is hoped that these results are indicative of the ability of the rainshaft model to simulate the various aspects of the evolution of raindrop spectra and rainfall.

Acknowledgments. One of the authors (GF) wishes to acknowledge support received from the Joseph Buchmann Fund during the course of his doctoral studies.

REFERENCES

Feingold, G. 1989: On the evolution of raindrop spectra and their effect on the atmosphere below cloud base: Numerical models and comparisons with observations. Ph.D. thesis, Tel Aviv University, 159 pp.

——, and Z. Levin, 1986: The lognormal fit to raindrop spectra from frontal convective clouds in Israel. *J. Climate Appl. Meteor.*, **25,** 1346–1363.

——, S. Tzivion and Z. Levin, 1991: The evolution of raindrop spectra: Part III. Downdraft generation in an axisymmetrical model. *J. Atmos. Sci.*, **48,** 315–330.

Gillespie, J. R., and R. List, 1978/79: Effects of collision induced breakup on drop-size distributions in steady-state rain shafts. *Pure Appl. Geophys.*, **117,** 599–626.

Gori, E. G., and J. Joss, 1980: Changes of shape of raindrop size distributions simultaneously observed along a mountain slope. *J. Rech. Atmos.*, **14,** 289–300.

Joss, J., and A. Waldvogel, 1967: Ein Spektrograph fur niederschlagstrophen mit automatischer auswertung. *Pure Appl. Geophys.*, **68,** 240–246.

——, and ——, 1977: Comments on "some observations on the Joss–Waldvogel rainfall distrometer." *J. Appl. Meteor.*, **16,** 112–113.

——, and E. G. Gori, 1978: Shapes of raindrop size distributions. *J. Appl. Meteor.*, **17,** 1054–1061.

Kinnell, P. I. A., 1976: Some observations on the Joss–Waldvogel rainfall disdrometer. *J. Appl. Meteor.*, **15,** 499–502.

List, R., N. R. Donaldson and R. E. Stewart, 1987: Temporal evolution of drop spectra to collisional equilibrium in steady and pulsating rain. *J. Atmos. Sci.*, **44,** 362–372.

List, R., 1988: A linear radar reflectivity–rain rate relationship for steady tropical rain. *J. Atmos. Sci.*, **45,** 3564–3572.

Rogers, R. R., 1989: Raindrop collision rates. *J. Atmos. Sci.*, **46,** 2469–2472.

Schumann, T., B. Zinder and A. Waldvogel, 1988: Aerosol and hydrometeor concentrations and their chemical composition during winter precipitation along a mountain slope—I. Temporal evolution of the aerosol, microphysical, and meteorological conditions. *Atmos. Environ.*, **22,** 1443–1459.

Sheppard, B. E., 1990: Effect of irregularities in the diameter classification of raindrops by the Joss–Waldvogel disdrometer. *J. Atmos. Oceanic. Technol.*, **7,** 180–183.

Srivastava, R. C., 1971: Size distribution of raindrops generated by their breakup and coalescence. *J. Atmos. Sci.*, **28,** 410–415.

Steiner, M., and A. Waldvogel, 1987: Peaks in raindrop size distributions. *J. Atmos. Sci.*, **44,** 3127–3133.

Tzivion, S., G. Feingold and Z. Levin, 1989: The evolution of raindrop spectra. II: Collisional collection–breakup and evaporation in a rainshaft. *J. Atmos. Sci.*, **46,** 3312–3327.

Valdez, M. P., and K. C. Young, 1985: Number fluxes in equilibrium raindrop populations: A Markov chain analysis. *J. Atmos. Sci.*, **42,** 1024–1036.

Willis, P. T., 1984: Functional fits to some observed drop-size distributions and parameterization of rain. *J. Atmos. Sci.*, **41,** 1648–1161.